MSEL
Modelling in Science Education and Learning

Modelling in Science Education and Learning
Volume 8(2), 2015 DOI: 10.4995/msel.2015.3523.
Instituto Universitario de Matemática Pura y Aplicada
Universitat Politècnica de València

A Teaching Experience: Aeroelasticity and the Finite Element Method

Una Experiencia Docente: Aeroelasticidad y el Método de los Elementos Finitos

Mario Lázaro
Universitat Politècnica de València
malana@mes.upv.es

Abstract

The aeroelastic modelling of aircraft structures is a fundamental area for the students of Aerospace Engineering Degree. This subject has a strongly multidisciplinary character and involves other several subjects like mechanics, vibrations, aerodynamics, structural analysis. Consequently, the students find stimulating the challenge of merging their knowledge at different areas. In this paper, a teaching experience on the solution of the aeroelastic problem of a 3D-wing through six different computer tasks is presented. The main objective is to attempt a relatively complex problem using a simple version of the Finite Element Method with only four degrees of freedom. The students begin creating the shape functions of the discrete model and finish solving the flutter instability problem.

La modelización aeroelástica de estructuras aeronáuticas es una materia fundamental en la formación de estudiantes de Grado de Ingeniería Aeroespacial. Esta materia tiene es multidisciplinar e involucra diferentes asignaturas vistas durante los estudios como mecánica, vibraciones, aerodinámica o estructuras. Por ello, los estudiantes encuentran estimulante el reto de fusionar sus conocimientos en diferentes areas en una sola asignatura. En este artículo se presenta una experiencia docente en la que se busca resolver el problema aeroelástico de un ala a través de 6 prácticas informáticas. El objetivo es poder abordar un problema tridimensional a priori relativamente complejo con una herramienta de gran utilidad en la mecánica computacional como es el método de los elementos finitos. Los estudiantes comienzan creando las funciones de forma para el modelo discreto y acaban resolviendo el problema de inestabilidad dinámica, el flameo

Keywords: aeroelasticity, finite element method, wing, bending, torsion, divergence, flutter, aerodynamics, vibrations
Palabras clave: aeroelasticidad, método elementos finitos, ala, flexión, torsión, divergencia, flameo, aerodinámica, vibraciones

Modelling in Science Education and Learning
http://polipapers.upv.es/index.php/MSEL

1 Introduction

Aeroelasticity, read as a subject within Aerospace Engineering Degree, is not usually coursed by students up to fourth course (7th or 8th semester). The reason is simple: it is maybe one of most multidisciplinary subjects since it relates several areas in mechanics: Rigid-Solid Dynamics, Aerodynamics, Structural Mechanics, Vibrations and Flight Mechanics. Arthur Collar (1947) defined Aeroelasticity as the science that studies the interaction between inertial, elastic and aerodynamic forces and he represented this interaction in a simple triangle (see Fig. 1, left).

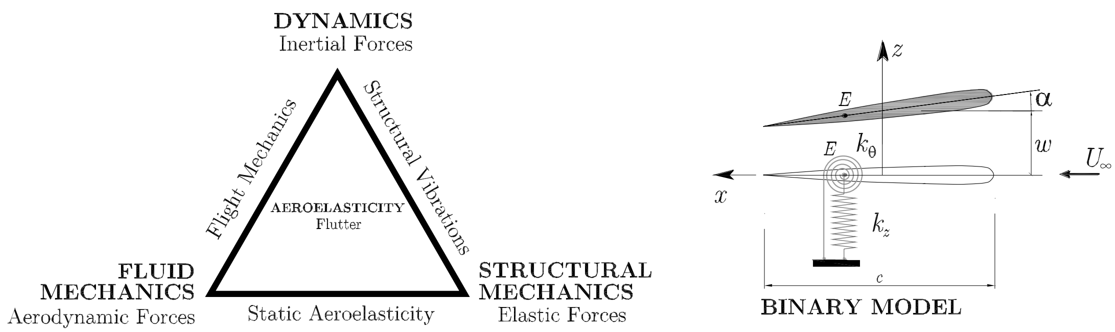

Figure 1: Left: Collar Triangle. “Aeroelasticity studies the interaction between inertial, elastic and aerodynamic forces”, Arthur Collar, 1947; Right: Airfoil binary model

In a first course of Aeroelasticiy two type of problems are usually presented: Instability and response problems. The objective of the first one is to obtain critical flight velocities which makes (statically or dynamically) the system unstable. The second one attempts the problem of obtaining the response of the system (in terms of elastic deformation or aerodynamic loads) for certain undercritical known velocity. From a teaching point of view, it is not advisable to introduce a complicated physical system, since as shown before any aeroelasticity model already involves several type of forces. Therefore, the named *binary model* with only 2 degrees of freedom (dof) is recommended to explain the main concepts. This model, shown in Fig. 1-right is formed by an airfoil attached to the ground with two springs simulating the bending and the torsional stiffness (Dowell, 2005; Edwards & Wieseman, 2008; Hancock et al., 1985). If the motion equations of the binary model can be expressed as a discrete system, the motion equations of 3D wing should be written in terms of partial differential equations, because deformation of airfoils depend now on the space coordinate and on time. Addressing this problem using differential equations in the space coordinates requires additionally concepts in Mathematics and at the same time, the physical insight of the problem can partially be lost. Although analytical solutions of the aeroelastic 3D problems are studied in the bibliography (Balakrishnan, 2012; Fung, 1993) we think that they should not be a priority for a under-graduate student.

The challenge is then is to attempt the aeroelastic problem of 3D wings but avoiding partial differential equations. In this paper we propose to obtain solutions discretizing the continuous by using the Finite Element Method. The process is carried out in six tasks from the model building to the calculation of the flutter instability. Here the six task with their main objectives are listed

Task 1. Finite elements model and shape functions.

Task 2. Strain energy and the stiffness matrix.

Task 3. Static aeroelasticity. Divergence and aeordynamic load distribution.

Task 4. The free-vibrations problem and the mass matrix.

Task 5. Dynamic aeroelasticity (I): unsteady aerodynamics.

Task 6. Dynamic aeroelasticity (II): flutter instability.

The final objective is to derive the discrete system of motion differential equations (in time) and to solve the flutter eigenvalue problem. For that, each task is divided in different sub-objectives usually focused on the computation of the different involved matrices and on the interpretation of the results. The duration of each task is between 1.5 and 2 hours. The students must upload the results at the end of the session in electronic form (Wolfram Mathematica© or Matlab© files).

We will see that just with four dofs, a relatively complex problem (the aeroelastic vibrations of a real wing) can be modeled. In addition, the physical interpretation of the results is easily available using the useful graphical tools of Mathematica and Matlab.

2 Problem definition

Before to present the different tasks we define the geometry and variables of the problem. Consider a straight wing, clamped at the root and free at the tip. In this point the main geometric and mechanic properties of the wing will be presented. Fig. 2 shows a 3D general overview of the wing with mid-span l and the 3-node finite element used for its modelling. The x–axis has the same direction as flow direction with velocity U_∞. y–axis coincides with elastic axis (middle point of chord) so that the wing surface is symmetric respect to this axis. Thus, z–axis is consequently upwards. The mid-chord $b(y)$ and stiffness properties —bending, $EI(y)$ and torsional, $GJ(y)$— are assumed to be variables in wingspan. In the derivation of the mathematical expressions non-dimensional geometric variables will be used, thus we define $\xi = x/b_0$ and $\eta = y/l$.

The unknown variables of the problem are expressed in terms of the following functions

- Heave motion: $w(\eta, t)$ defines the vertical displacement of elastic axis ($x = 0$), of the airfoil located at $y = \eta l$. Positive upwards.

- Pitch rotation: $\theta(\eta, t)$ is the rotation of the airfoil located at coordinate $y = \eta l$, positive in y direction.

Both functions allows to obtain the displacement of any point of the mid-plane of the wing with coordinates (x, y), expressed as a surface $z(x, y)$. The general formulation of the motion equations of the wing result in a system of two coupled partial differential equations in functions $w(y, t)$ and $\theta(y, t)$. But as said before, the objectives of these tasks are not to attempt the problem using differential equations in the space coordinates. Instead, we will use polynomial approximations for $w(\eta, t)$ and $\theta(\eta, t)$, which will allows us to work in a discrete domain rather than a continuous one.

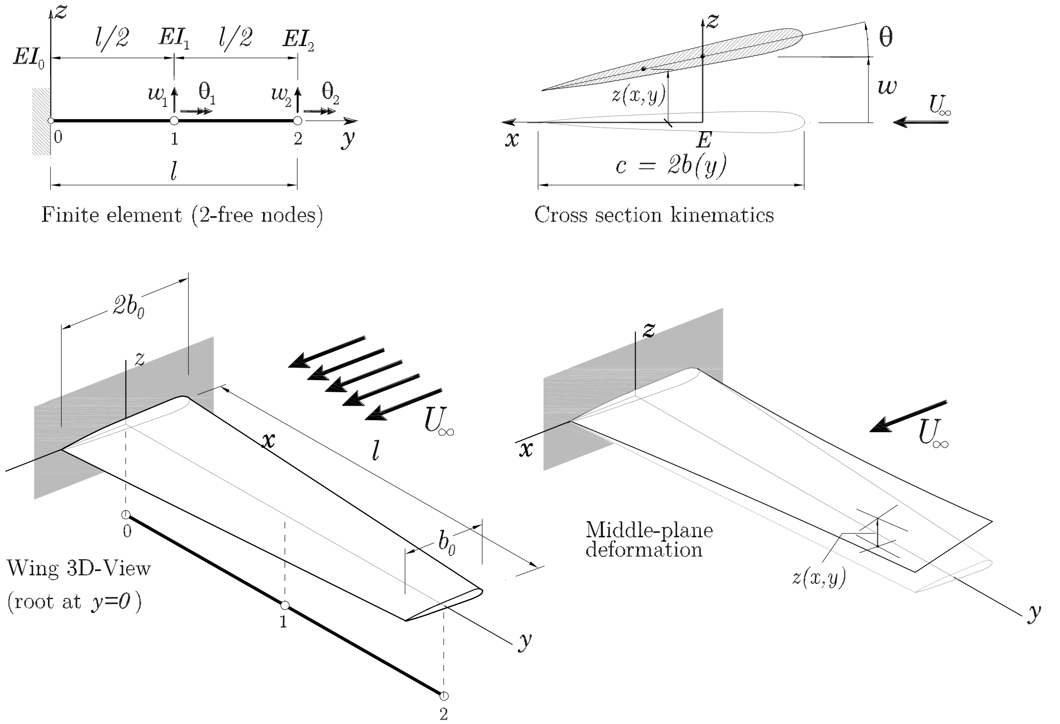

Figure 2: Geometry and 3-node finite element definition of a clamped-free wing

3 Task 1: Finite elements model and shape functions

The objective of this task is to create a finite element model (FEM) necessary to the aeroelastic analysis. In addition, the students learn the new notation and practice with the matrix formulation. Particularly, the points to be solved are

1. Using just one finite element, obtain the shape functions for $w(y)$ associated to the nodal displacements (w_1 and w_2), and those for $\theta(y)$ associated to the nodal rotations (θ_1 and θ_2). Plot the results.

2. Define a unique array $\mathbf{u}$ containing all (non-dimensional) degrees of freedom and construct both matrices $\mathbf{N}_w(\eta)$ and $\mathbf{N}_\theta(\eta)$ so that

$$w(\eta) = b_0 \, \mathbf{N}_w^T(\eta) \, \mathbf{u} \quad , \quad \theta(\eta) = \mathbf{N}_\theta^T(\eta) \, \mathbf{u}$$

   where $\eta = y/l$.

3.1 The shape functions

A finite element model basically discretizes the continuum in several *pieces* jointed by nodes. The challenge of solving the problem from its differential formulation is replaced by a not so pretentious one: to solve just at the nodes. The solution at all remainder points will be interpolated by a special type of functions (in most cases polynomials) named *shape functions*. More details on the fundamentals of the FEM and its applications can be found in the reference (Zienkiewicz & Taylor, 2005).. We describe in this point how to construct this functions for our particular case.

	$\eta = 0$	$\eta = 1/2$	$\eta = 1$
Heave displacement, $w(\eta)$	$w(0) = 0$, $w'(0) = 0$	$w(1/2) = w_1$	$w(1) = w_2$
Pitch angle, $\theta(\eta)$	$\theta(0) = 0$	$\theta(1/2) = \theta_1$	$\theta(1) = \theta_2$

Table 1: Restrictions to be verified by proposed polynomials for $w(\eta)$ and $\theta(\eta)$

The movements of the wing are governed by two functions: the vertical displacement of y-axis, denoted by $w(y)$, and the twist angle of y-axis, named $\theta(y)$. These functions are assumed to be dependent on the y coordinate, or in non-dimensional terms on the η variable, with $\eta = y/l$. At the end of the point, the introduction of the time as another independent variable will be explained, although it only be used in dynamic problems (Task 4 and following). Since we are interested in teaching the method and not solving with accuracy the problem, we use just one element with three nodes to model our wing (see Fig. 2). Node 0 is the clamped constraint at the wing-root, nodes 1 and 2 are located at the middle span and at the wingtip, respectively. Nodes 1 and 2 are free, that means they can move upwards and rotate in y-direction. However, node 0 is fixed, without displacements and rotations. We denote by w_1, w_2, θ_1, θ_2 to the vertical displacements and y-rotations of nodes 1 and 2, respectively. In the approximated solution for $w(\eta)$ and $\theta(\eta)$ the previous conditions should be considered, something that will inform us on the polynomial degree we need. We summarize the conditions to be imposed to $w(\eta)$ and $\theta(\eta)$ in the Table 1.

Since we have 4 conditions for the heave displacement we will approximate $w(\eta)$ by a 3–degree polynomial, which can be written as

$$w(\eta) \approx a_0 + a_1\eta + a_2\eta^2 + a_3\eta^3 \tag{1}$$

The four conditions of Table 1 generates a linear system of 4 equations with 4 unknowns $\{a_0, a_1, a_2, a_3\}$ whose solution is

$$a_0 = 0\ ,\ a_1 = 0\ ,\ a_2 = 8w_1 - w_2\ ,\ a_3 = -8w_1 + 2w_2 \tag{2}$$

Introducing this result in Eq. (1) and ordering

$$w(\eta) \approx \left(8\eta^2 - 8\eta^3\right) w_1 + \left(-\eta^2 + 2\eta^3\right) w_2 \equiv N_{w1}(\eta)w_1 + N_{w2}(\eta)w_2 \tag{3}$$

The two functions $N_{w1}(\eta)$, $N_{w2}(\eta)$ are named *shape functions* because in a way the are able to transform the node solution in a continuous shape. Since the shape functions are a priori known, to introduce $w(\eta)$ in the motion equations should reduce the problem to the discrete unknowns w_1, w_2.

For the function $\theta(\eta)$ the procedure is the same although only three conditions are imposed. This leads to a 2–degree interpolation polynomial. After some operations we obtain

$$\theta(\eta) \approx \left(4\eta - 4\eta^2\right) \theta_1 + \left(2\eta^2 - \eta\right) \theta_2 \equiv N_{\theta 1}(\eta)\theta_1 + N_{\theta 2}(\eta)\theta_2 \tag{4}$$

Fig. 3 shows the shape functions. Note that each function verifies the boundary conditions, that is, they are particular valid solutions of the problem. In addition, N_{w1} takes the value 1 at node 1 and 0 at node 2. On the contrary, $N_{w2}(1) = 1$ and $N_{w2}(1/2) = 0$. The same occurs for $N_{\theta 1}$, $N_{\theta 2}$ and in general for any shape function we construct under similar conditions.

3.2 Compact expressions and matrix notation

We define the following 4th order dimensionless array

$$\mathbf{u} = \{w_1/b_0, \theta_1, w_2/b_0, \theta_2\}^T \tag{5}$$

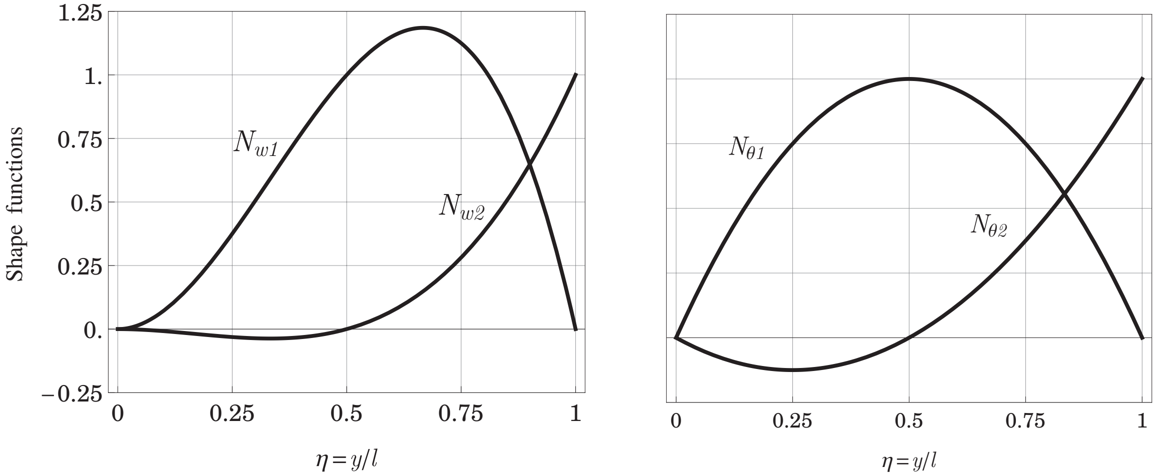

Figure 3: Left: shape functions associated to the vertical displacements w_1 and w_2. Right: shape functions associated to the twist rotations θ_1 and θ_2

where b_0 is the mid-chord at the wing-root $\eta = 0$. This array (in column) contains the 4 (dimensionless) degrees of freedom (dof) of our problem. Both, heave and pitch variables are included since aeroelastic problems are concerned on the bending-torsional coupling problems. These four dof control the state of our system in each time. In fact, this array will be function of time in the dynamic problems. In order to obtain compact forms of strain and kinetic energies we look for certain matrices $\mathbf{N}_w(\eta)$ and $\mathbf{N}_\theta(\eta)$ which transform $\mathbf{u}$ into $w(\eta)$ and $\theta(\eta)$, so that

$$w(\eta) = b_0\, \mathbf{N}_w^T(\eta)\, \mathbf{u} \quad , \quad \theta(\eta) = \mathbf{N}_\theta^T(\eta)\, \mathbf{u} \tag{6}$$

The solution this question is straightforward. Thus, for example for $w(\eta)$ we have

$$\begin{aligned} w(\eta) &= N_{w1}(\eta) w_1 + N_{w2}(\eta) w_2 \\ &= b_0 \left(N_{w1}(\eta) \frac{w_1}{b_0} + 0 \cdot \theta_1 + N_{w2}(\eta) \frac{w_2}{b_0} + 0 \cdot \theta_2 \right) \\ &\equiv b_0\, \mathbf{N}_w^T(\eta) \mathbf{u} \end{aligned} \tag{7}$$

In fact, as pointed above, w does not only depend on the y coordinate, but also on the time t in a dynamic problem. Rigorously, we should write $w(\eta, t) = b\, \mathbf{N}_w(\eta)\mathbf{u}(t)$. The time notation t will be omitted in the static problems and will return to appear in those of dynamic nature.

We find a quite similar form for torsional rotations in terms of the dof's

$$\theta(\eta, t) = N_{\theta 1}(\eta)\theta_1(t) + N_{\theta 2}(\eta)\theta_2(t) \equiv \mathbf{N}_\theta^T(\eta)\mathbf{u}(t) \tag{8}$$

where $\mathbf{N}_\theta(\eta) = \{0, N_{\theta 1}(\eta), 0, N_{\theta 2}(\eta)\}^T$. The forms (7) and (8) will be repeatedly use in the rest of the tasks.

It becomes also of interest to know the vertical displacement of any point of the middle-plane, $z(x, y)$, from certain values of the dofs, $\mathbf{u}$. In other words, we want to know the deformed surface $z(x, y)$ of middle-plane of the wing when the array of dofs, $\mathbf{u}$, is known. From the airfoil kinematics (see Fig. 2) we have

$$z(x, y) = w(y) - x\, \theta(y) \tag{9}$$

Now, using the dimensionless coordinates $\xi = x/b_0$ and $\eta = y/l$ and the shape functions defined above in Eqs. (7),(8),

$$z(\xi,\eta) = b_0 \mathbf{N}_w^T(\eta)\mathbf{u} - \xi\, b_0\, \mathbf{N}_\theta^T(\eta)\mathbf{u} = b_0 \left[\mathbf{N}_w^T(\eta) - \xi\, \mathbf{N}_\theta^T(\eta)\right]\mathbf{u} \equiv b_0\, \mathbf{N}_z^T(\xi,\eta)\,\mathbf{u} \tag{10}$$

Thus, the matrix

$$\mathbf{N}_z(\xi,\eta) = \mathbf{N}_w(\eta) - \xi\, \mathbf{N}_\theta(\eta) = \{N_{w1}(\eta), -\xi\, N_{\theta 1}(\eta), N_{w2}(\eta), -\xi\, N_{\theta 2}(\eta)\}^T \tag{11}$$

transform the dofs into the vertical displacement at point (ξ,η).

4 Task 2: Strain energy and the stiffness matrix

The information about the linear-elastic properties is contained within the elastic strain energy. The main objective is to obtain this energy as function of dofs and deduce the stiffness matrix. The solution of a static case under certain imposed load case is also proposed. The objectives of this task can be addressed solving the following two points

1. Calculate the stiffness matrix $\mathbf{K}$, separating those parts associated to bending $\mathbf{K}_b$ and torsional $\mathbf{K}_t$ behavior

2. Assuming a vertical load in one of the free corners of the wing, calculate the displacement in the loaded corner and graphically represent the deformed surface (3D).

4.1 Stiffness matrix

The strain energy is part of the Lagrange equations and contains the potential energy of those elastic parts. The stiffness of our structure is located in the elastic axis, which coincides with y-axis in $0 \le y \le l$. The wing can be deformed under bending and torsional effects. The strain energy concept of a beam can be found in any course of Structural Mechanics and can be expressed in terms of the *strains* of a beam under bending and torsional behavior: the curvatures $\partial^2 w/\partial y^2$ and the unit angle $\partial\theta/\partial y$ (Megson, 2010)

$$\mathcal{U} = \frac{1}{2}\int_0^l EI(y)\left(\frac{\partial^2 w}{\partial y^2}\right)^2 dy + \frac{1}{2}\int_0^l GJ(y)\left(\frac{\partial \theta}{\partial y}\right)^2 dy \equiv \mathcal{U}_b + \mathcal{U}_t \tag{12}$$

where $\mathcal{U}_b, \mathcal{U}_t$ are the bending and torsional strain energy. The stiffness matrices associated to the bending and torsional behavior will separately be obtained. Before But before, we will give a useful mathematical property that will help us in the derivation of matrix expressions. Let us consider two scalar magnitudes, p and q, expressed in terms of both scalar product as

$$p = \mathbf{P}^T\mathbf{x}\ , \quad q = \mathbf{Q}^T\mathbf{y} \tag{13}$$

with $\mathbf{P},\mathbf{Q},\mathbf{x},\mathbf{y} \in \mathbb{R}^n$ are n–order arrays in column. Then the product pq can be indistinctly calculated as

$$\begin{aligned} pq &= p^T q = \mathbf{x}^T\mathbf{P}\mathbf{Q}^T\mathbf{y} \equiv \mathbf{x}^T\mathbf{R}\,\mathbf{y} && (14)\\ &= q^T p = \mathbf{y}^T\mathbf{Q}\mathbf{P}^T\mathbf{x} \equiv \mathbf{y}^T\mathbf{S}\,\mathbf{x} && (15)\end{aligned}$$

where $\mathbf{R}$ and $\mathbf{S}$ are $n \times n$ square matrices so that $\mathbf{R} = \mathbf{S}^T = \mathbf{P}\mathbf{Q}^T$. This property will be repeatedly used along the different tasks

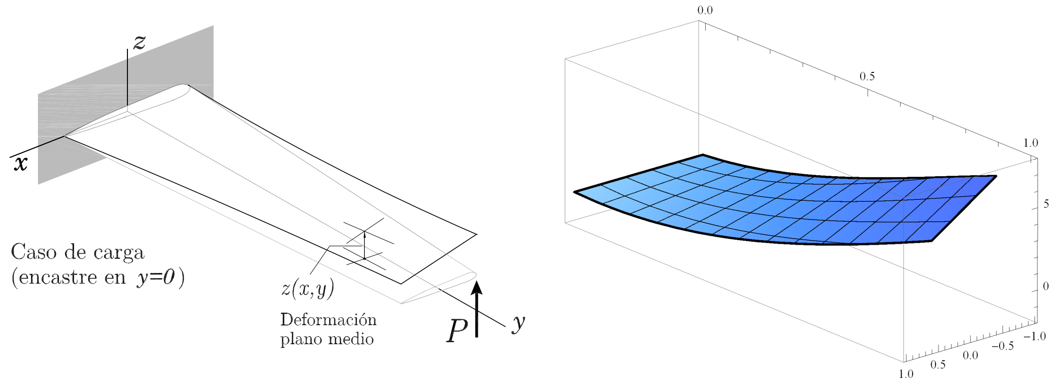

Figure 4: Elastic deformation due to a eccentric point-load at wingtip. Load case (left) and wing middle-plane deformed, calculated with Mathematica (right)

Returning to the equations of strain energy, both the curvatures $\partial^2 w/\partial y^2$ and the unit rotation $\partial\theta/\partial y$ can be expressed as scalar products. Indeed, using Eqs. (6), we have

$$\frac{\partial^2 w}{\partial y^2} = \frac{1}{l^2}\frac{\partial^2 w}{\partial \eta^2} = \frac{1}{l^2}\frac{\mathrm{d}^2\mathbf{N}_w^T}{\mathrm{d}\eta^2}\,\mathbf{u}\ , \quad \frac{\partial\theta}{\partial y} = \frac{1}{l}\frac{\partial\theta}{\partial\eta} = \frac{1}{l}\frac{\mathrm{d}\mathbf{N}_\theta^T}{\mathrm{d}y}\,\mathbf{u} \tag{16}$$

Using these matrix expressions we can derive a quadratic form for both the bending and torsional strain energies.

$$\begin{aligned}
\mathcal{U}_b &= \frac{1}{2}\int_0^l EI\left(\frac{\partial^2 w}{\partial y^2}\right)^2 dy = \frac{1}{2}\int_0^1 \frac{EI}{l^3}\left(\frac{\partial^2 w}{\partial \eta^2}\right)^2 d\eta = \frac{1}{2}\int_0^1 \frac{EI}{l^3}\left(\frac{\partial^2 w}{\partial \eta^2}\right)^T\left(\frac{\partial^2 w}{\partial \eta^2}\right) d\eta \\
&= \frac{1}{2}\int_0^1 \frac{b_0^2 EI(\eta)}{l^3}\left(\mathbf{u}^T\frac{\mathrm{d}^2\mathbf{N}_w}{\mathrm{d}\eta^2}\right)\left(\frac{\mathrm{d}^2\mathbf{N}_w^T}{\mathrm{d}\eta^2}\mathbf{u}\right) d\eta = \frac{1}{2}\mathbf{u}^T\left(\int_0^1 \frac{b_0^2 EI(\eta)}{l^3}\frac{\mathrm{d}^2\mathbf{N}_w}{\mathrm{d}\eta^2}\frac{\mathrm{d}^2\mathbf{N}_w^T}{\mathrm{d}\eta^2}\,d\eta\right)\mathbf{u} \\
&\equiv \frac{1}{2}\mathbf{u}^T\,\mathbf{K}_b\,\mathbf{u}
\end{aligned} \tag{17}$$

$$\begin{aligned}
\mathcal{U}_t &= \frac{1}{2}\int_0^l GJ\left(\frac{\partial\theta}{\partial y}\right)^2 dy = \frac{1}{2}\int_0^1 \frac{GJ}{l}\left(\frac{\partial\theta}{\partial\eta}\right)^2 d\eta = \frac{1}{2}\int_0^1 \frac{GJ}{l}\left(\frac{\partial\theta}{\partial\eta}\right)^T\left(\frac{\partial\theta}{\partial\eta}\right) d\eta \\
&= \frac{1}{2}\int_0^1 \frac{GJ(\eta)}{l}\left(\mathbf{u}^T\frac{\mathrm{d}\mathbf{N}_\theta}{\mathrm{d}\eta}\right)\left(\frac{\mathrm{d}\mathbf{N}_\theta^T}{\mathrm{d}\eta}\mathbf{u}\right) d\eta = \frac{1}{2}\mathbf{u}^T\left(\int_0^1 \frac{GJ(\eta)}{l}\frac{\mathrm{d}\mathbf{N}_\theta}{\mathrm{d}\eta}\frac{\mathrm{d}\mathbf{N}_\theta^T}{\mathrm{d}\eta}\,d\eta\right)\mathbf{u} \\
&\equiv \frac{1}{2}\mathbf{u}^T\,\mathbf{K}_t\,\mathbf{u}
\end{aligned} \tag{18}$$

where

$$\mathbf{K}_b = \int_0^1 \frac{b_0^2 EI(\eta)}{l^3}\frac{\mathrm{d}^2\mathbf{N}_w}{\mathrm{d}\eta^2}\frac{\mathrm{d}^2\mathbf{N}_w^T}{\mathrm{d}\eta^2}\,d\eta\ , \quad \mathbf{K}_t = \int_0^1 \frac{GJ(\eta)}{l}\frac{\mathrm{d}\mathbf{N}_\theta}{\mathrm{d}\eta}\frac{\mathrm{d}\mathbf{N}_\theta^T}{\mathrm{d}\eta}\,d\eta \tag{19}$$

are respectively the bending and torsional stiffness matrices, that can be calculated simply integrating the shape functions derivatives if certain mechanical properties variation for $EI(\eta)$, $GJ(\eta)$ are given. The total stiffness matrix of the system result of the sum

$$\mathbf{K} = \mathbf{K}_b + \mathbf{K}_t \tag{20}$$

4.2 Solution of a static problem

Using the previous result the students can also apply their knowledge on structural analysis calculating the elastic deformation of the wing given a static load case. Consider a point-load

P located at (x_p, y_p). The Lagrange equations for discrete mechanical systems will be used along the different tasks to derive the motion equations. Since this problem involves only static forces, the system of equations is

$$\frac{\partial \mathcal{U}}{\partial \mathbf{u}} = \mathbf{Q} \tag{21}$$

where $\partial/\partial\mathbf{u}$ denotes the gradient operator (in column) respect to the variables listed by $\mathbf{u}$ and $\mathbf{Q}$ represents the generalized forces associated to $\mathbf{u}$, calculated from the virtual work done by the external forces (Wright & Cooper, 2007). It is assumed that students are familiarized with the concept of generalized forces, which repeatedly appears in the Lagrange equations. This simple load case allows us to recycle this concept. Thus, let the system be at certain position given by $\mathbf{u}$ and under the force P. Let us assume that the dofs undergoes a virtual variation $\delta\mathbf{u}$, giving as a result virtual displacements at any point. Thus, the point where P is located, say z_P, moves to $z_P + \delta z_P$ so that the virtual work becomes $\delta\mathcal{W} = P\,\delta z_P$. The generalized forces are those magnitudes which multiplied by the dofs virtual variation give as result the virtual work. Therefore, we are looking for expressing the virtual work as the scalar product $\delta\mathcal{W} = \delta\mathbf{u}^T\mathbf{Q}$. For that, we know (see Task 1, Eq. (10)) that the displacement of any point located at (ξ,η) is $z(\xi,\eta) = b_0\mathbf{N}_z^T(\xi,\eta)\mathbf{u}$. In particular, at point $P(\xi_P,\eta_P)$ we have

$$z_P = b_0\mathbf{N}_z^T(\xi_P,\eta_P)\mathbf{u} \equiv b_0\mathbf{N}_P^T\,\mathbf{u}$$

Therefore, the virtual displacement is $\delta z_P = b_0\mathbf{N}_P^T\,\delta\mathbf{u}$, and the virtual work results

$$\delta\mathcal{W} = P\,\delta z_P = \delta z_P^T\,P = \delta\mathbf{u}^T\,(b_0\,\mathbf{N}_P\,P) = \delta\mathbf{u}^T\,\mathbf{Q} \tag{22}$$

whence $\mathbf{Q} = Pb_0\,\mathbf{N}_P$.

Before deriving the system of equations to obtain the response due to P, a useful property will be presented: If $\mathcal{A}(\mathbf{x}) = \mathbf{x}^T\mathbf{A}\mathbf{x}/2$ is a generic quadratic form, then the gradient operator is

$$\frac{\partial\mathcal{A}}{\partial\mathbf{x}} = \frac{\partial}{\partial\mathbf{x}}\left(\frac{1}{2}\mathbf{x}^T\mathbf{A}\mathbf{x}\right) = \frac{1}{2}\left(\mathbf{A}+\mathbf{A}^T\right)\mathbf{x} \tag{23}$$

Introducing the result for $\mathbf{Q}$ in Eq. (21) together with the expression of the strain energy $\mathcal{U}$, the dofs satisfy the following linear system of equations

$$\frac{\partial\mathcal{U}}{\partial\mathbf{u}} = \frac{\partial}{\partial\mathbf{u}}\left(\frac{1}{2}\mathbf{u}^T\,\mathbf{K}\,\mathbf{u}\right) = \frac{1}{2}\left(\mathbf{K}+\mathbf{K}^T\right)\mathbf{u} = \mathbf{K}\,\mathbf{u} = \mathbf{Q} = Pb_0\,\mathbf{N}_P \tag{24}$$

resulting $\mathbf{u} = Pb_0\,\mathbf{K}^{-1}\,\mathbf{N}_P$. In Eq. (24) we have used the symmetry of $\mathbf{K}$. The deformed surface of the wing can already be obtained using the Eq. (10)

$$z(\xi,\eta) = b_0\,\mathbf{N}_z^T(\xi,\eta)\,\mathbf{u} = b_0^2P\,\mathbf{N}_z^T(\xi,\eta)\,\mathbf{K}^{-1}\,\mathbf{N}_P \tag{25}$$

This surface has been plotted in Fig. 4 using Wolfram Mathematica©, with P located at a corner of the wing-tip. In particular, the displacement at the loaded point is

$$z_P = b_0^2P\,\mathbf{N}_P^T\,\mathbf{K}^{-1}\,\mathbf{N}_P$$

.

This task allow the students to introduce in the basis of the finite element method to structural analysis. The different items are solved using Wolfram Mathematica©, with which students are able to obtain and represent solutions even with variable mechanical properties.

5 Task 3: Static aeroelasticity

Static aeroelasticity is usually the first problem seen by students coupling elastic and aerodynamic forces. In this task, the model involving both types of forces is described; for that, it is necessary to express the aerodynamic model in terms of the named generalized forces. The objectives are summarized in the following items

1. Obtain the generalized forces associated to the aerodynamics associated to the dofs $\mathbf{u}$.
2. Calculate the lift–force distribution along the wing

5.1 Generalized forces from steady aerodynamics

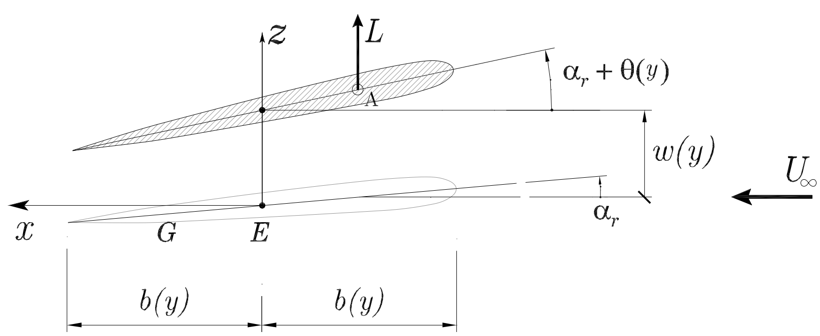

Figure 5: Rigid and elastic rotation angle of a arbitrary airfoil located at $y = \eta l$.

The aerodynamic forces are obtained assuming lightly perturbed incompressible potential flow, valid for low angles of attack. We denote by $L(y)$ to the lift force in a generic airfoil located at $y \in [0, l]$. This force per unit-length can be calculated following the classic aerdoynamic theory of slender lifting surfaces (Anderson, 2001; Meseguer & Sanz-Andrés, 2010) and can be expressed as

$$L(y) = \frac{1}{2}\rho_\infty U_\infty^2 S_w C_L \tag{26}$$

Students are usually familiarized with this theory since they have previously coursed Aerdoynamics. Therefore, they have already heard about terms like lift force, aerodynamic center, pitch moment, dynamic pressure or lif coefficent. In spite of the flow velocity we work in static aeroelasticity with the dynamic presure $q = \rho_\infty U_\infty^2/2$. The force shown in Eq. (26) is located at the aerdynamic center in a particular section. Hence S_w represents the lifting surface per unit-length (units of FL^{-1}), so that $S_w = 2b(y)$. Finally, assuming low angle of attack the lift coefficient is evaluated at the straight part of the lift curve resulting $C_L \approx C_{L\alpha}\,\alpha(y)$. In our study case, we consider that the total angle of attack is sum of certain geometric angle (constant), plus the additional rotation angle, $\theta(y)$, due to the torsional elastic deformation (see Fig. 5).

$$\alpha(y) = \alpha_r + \theta(y) \tag{27}$$

Using the shape functions seen in Task 1, Eq. 8 we have $\theta(\eta) = \mathbf{N}_\theta^T(\eta)\mathbf{u}$ (using the dimensionless coordinate $\eta = y/l$). Consequently,

$$L(\eta) = q\,2b(\eta)\,C_{L\alpha}\;(\alpha_r + \theta) = q\,2b(\eta)\,C_{L\alpha}\,\mathbf{N}_\theta^T(\eta)\mathbf{u} + q\,2b(\eta)\,C_{L\alpha}\,\alpha_r \tag{28}$$

This equation relates the dofs with the lift distribution along the span.

The generalized aerodynamic force Q_j is associated to the jth dof and is, by definition, the virtual work done by the external forces por unit of variation of the jth dof. We denote by z_A the vertical displacement of the aerodynamic center for certain values of $\mathbf{u}$. Thus, the virtual work done by the lift distribution for a virtual variation of the dofs, $\delta\mathbf{u}$ is

$$\delta\mathcal{W} = \int_{y=0}^{l} L(y)\,\delta z_A\,dy \tag{29}$$

The aerodynamic center of a generic airfoil is located at a quarter-chord of the leading edge; its x-coordinate is then $x = -b(y)/2$ and its displacement $z_A(y) = z\left[-b(y)/2, y\right]$. Using the Eq. (10) in terms of the dimensionless coordinates we have

$$z_A(\eta) = z\left(-\frac{b(\eta)}{2b_0}, \eta\right) = b_0 \mathbf{N}_z\left(-b(\eta)/b_0, \eta\right)\,\mathbf{u} \equiv b_0 \mathbf{N}_A(\eta)\,\mathbf{u} \tag{30}$$

The variation $\delta\mathbf{u}$ leads to a variation $\delta z_A(\eta) = \mathbf{N}_A^T(\eta)\delta\mathbf{u}$ and the total virtual work done by the aerodynamic forces along the span is

$$\begin{aligned}
\delta\mathcal{W} &= \int_{y=0}^{1} L(y)\,\delta z_A(y) dy = \int_{\eta=0}^{1} l\,\delta z_A^T(\eta) L(\eta)\,d\eta \\
&= \int_{\eta=0}^{1} l\,\delta\mathbf{u}^T \mathbf{N}_A(\eta)\left(q\,2b(\eta)\,C_{L\alpha}\,\mathbf{N}_\theta^T(\eta)\mathbf{u} + q\,2b(\eta)\,C_{L\alpha}\,\alpha_r\right) \\
&= \delta\mathbf{u}\left(q\int_{\eta=0}^{1} 2lb(\eta)\,C_{L\alpha}\,\mathbf{N}_A(\eta)\mathbf{N}_\theta^T(\eta)d\eta + q\,\alpha_r\int_{\eta=0}^{1} 2lb(\eta)\,C_{L\alpha}\,\mathbf{N}_A(\eta)\,d\eta\right) \\
&\equiv \delta\mathbf{u}^T\,\mathbf{Q}
\end{aligned} \tag{31}$$

whence, identifying it results

$$\mathbf{Q} = q\left(\int_{\eta=0}^{1} 2l\,b(\eta)\,C_{L\alpha}\,\mathbf{N}_A(\eta)\mathbf{N}_\theta^T(\eta)\,d\eta\right)\mathbf{u} + q\left(\int_{\eta=0}^{1} 2lb(\eta)\,C_{L\alpha}\,\mathbf{N}_A(\eta)\,d\eta\right)\alpha_r \equiv q\mathbf{A}\mathbf{u} + q\,\mathbf{a}\,\alpha_r \tag{32}$$

The matrix $\mathbf{A}$ relates the dofs of the system with the aerodynamic generalized forces and their entrees are usually named *Aerodynamic Influence Coefficients*, AIC (Wright & Cooper, 2007).

5.2 Divergence instability

The response of the dofs for certain value of the rigid-geometric angle α_r is solved using the Lagrange equations. Using again the strain energy $\mathcal{U} = \mathbf{u}^T\mathbf{K}\mathbf{u}/2$ and the generalized forces given by Eq. (32), we have

$$\frac{\partial\mathcal{U}}{\partial\mathbf{u}} = \mathbf{K}\,\mathbf{u} = q\mathbf{A}\mathbf{u} + q\,\mathbf{a}\,\alpha_r = \mathbf{Q} \tag{33}$$

resulting the linear system of equations

$$\mathbf{K}\mathbf{u} = q\mathbf{A}\mathbf{u} + q\,\mathbf{a}\,\alpha_r \tag{34}$$

and under the usual form presented for static aeroelastic problems

$$\left(\mathbf{K} - q\mathbf{A}\right)\mathbf{u} = \mathbf{f} \tag{35}$$

MODE	EXACT	FEM	ERROR (%)
q_1	$2.467q_r$	$2.486q_r$	0.76 %
q_2	$22.206q_r$	$32.18q_r$	45 %

Table 2: Comparison between exact and approximate divergence modes

Note that in the left term we leave the dofs-dependent part, while the right part $\mathbf{f} = q\,\mathbf{a}\,\alpha_r$ of the equation only shows dofs–independent forces. The latter can be proportional to the flow velocity (as in our study case) or, otherwise, it could be independent on U_∞ as (for instance) the generalized forces derived from the self-weight. The motion equation so written is the most general form for the aeroelastic static equations. This equations represent the response of a system whose stiffness is reduced by the effect of the aerodynamic flow. In fact, we could find some value of the velocity q for which the response was unbounded. These values of q necessary vanish the determinant of the matrix coefficients $\mathbf{K} - q\,\mathbf{A}$ and are solutions of the linear eigenvalue problem

$$(\mathbf{K} - q\mathbf{A})\,\mathbf{u} = \mathbf{0} \tag{36}$$

and the are named *divergence modes*. Among them, the lowest positive eigenvalue (if it exists) is usually named *divergence dynamic pressure* and the associated velocity, *divergence velocity*.

Let us consider a numerical example: a wing with uniform chord $2b$ and mechanical properties, EI, GJ, invariable along the span l. The stiffness and AIC matrices are then

$$\mathbf{K} = \frac{GJ}{l}\begin{bmatrix} 256\beta/\lambda^2 & 0 & -80\beta/\lambda^2 & 0 \\ 0 & 16/3 & 0 & -8/3 \\ -80\beta/\lambda^2 & 0 & 28\beta/\lambda^2 & 0 \\ 0 & -8/3 & 0 & 7/3 \end{bmatrix}, \quad \mathbf{A} = \frac{lb^2 C_{L\alpha}}{15}\begin{bmatrix} 0 & 16 & 0 & 4 \\ 0 & 8 & 0 & 1 \\ 0 & 2 & 0 & 7/2 \\ 0 & 1 & 0 & 2 \end{bmatrix} \tag{37}$$

where $\lambda = l/b$ and $\beta = EI/GJ$. The eigenvalues of Eq. (36) can be calculated solving the characteristic polynomial

$$\det\left[\mathbf{K} - q\mathbf{A}\right] = \frac{256\beta^2}{\lambda^4}\left[q(3q - 104q_r) + 240q_r^2\right] \;\rightarrow\; q_1 = 2.4859q_r\ ,\ q_2 = 32.18q_r \tag{38}$$

where $q_r = GJC_{L\alpha}/b^2l^2$ is a reference pressure. This equation has two roots but the problem has four dofs, so why? It seems to be a contradiction, since a linear eigenvalue problem with 4×4 matrices should also have four eigenvalues. Mathematically we note that $\mathbf{A}$ is singular, moreover its range is 2. This means that the $q = \infty$ is eigenvalue with multiplicity 2. Physically, the associated modes can be calculated solving the ill-conditioned linear system $\mathbf{Au} = \mathbf{0}$ resulting $\theta_1 = 0$ and $\theta_2 = 0$, that is any purely bending deformation is an eigenshape of the eigenvalue $q = \infty$. In other words, a straight wing never diverges under bending.

In order to validate the model we can compare the obtained results with the exact ones, available for this particular case solving the eigenvalue problem but in terms of differential equations. Thus, for a straight and uniform wing with chord $2b$, span l and torsional sectional stiffness GJ the sequence of exact eigenvalues is $q_n = \pi^2(1 + 2n)^2 q_r/4$ for $n = 0, 1, 2, \ldots$ (Balakrishnan, 2012). In the Table 2 the values for the two first modes are shown. The finite element model used for these tasks presents less than 1% in the evaluation of the divergence pressure. However, the error considerably increases for the second mode, something that has influence in the accuracy of the load distribution evaluated in the next point.

5.3 Lift distribution along deformable wings

Assuming that we fly under the divergence limit, we can calculate the extra-lift that appears on our wings due to the elastic deformation. Returning to the expression of $L(\eta)$ and replacing the response given by $\mathbf{u} = q\,(\mathbf{K} - q\mathbf{A})^{-1}\,\mathbf{a}\,\alpha_r$ we have

$$\begin{aligned} L(\eta) &= q\,2b(\eta)\,C_{L\alpha}\,(\alpha_r + \theta) \\ &= q\,2b(\eta)\,C_{L\alpha}\,\mathbf{N}_\theta^T(\eta)\mathbf{u} + q\,2b(\eta)\,C_{L\alpha}\,\alpha_r \\ &= q^2\,2b(\eta)\,C_{L\alpha}\,\mathbf{N}_\theta^T(\eta)\,(\mathbf{K} - q\mathbf{A})^{-1}\,\mathbf{a}\,\alpha_r + q\,2b(\eta)\,C_{L\alpha}\,\alpha_r \\ &= L_r(\eta)\,\left[1 + q\mathbf{N}_\theta^T(\eta)\,(\mathbf{K} - q\mathbf{A})^{-1}\,\mathbf{a}\right] \end{aligned} \tag{39}$$

where we have denoted by $L_r(\eta) = q\,2b(\eta)\,C_{L\alpha}\,\alpha_r$ to the lift distribution if the system would be completely rigid. Considering fixed all the parameters of the problem except the coordinate η and velocity q, the Eq. (28) gives provides the total force on the wing for each velocity (in terms of dynamic pressure). Since this extra lift is inversely proportional to the determinant $\det(\mathbf{K} - q\mathbf{A})$, if the velocity gets close to that of the divergence, the total lift tends to infinite. The validity of the obtained load distribution depends on the accuracy of the response $\mathbf{u}$. We have seen that the error at the second divergence mode is markedly higher than that of the first mode. Intuitively we could improve the model adding more dofs, specially if they were twist y-rotations, rather than vertical displacements. If fact, note that $L(\eta)$ is proportional to the shape functions associated to the rotation, so that somehow we can only reach a parabolic form for the load distribution. To achieve a higher accuracy level is linked to increase the polynomial order of the rotation shape functions involved in $\mathbf{N}_\theta^T(\eta)$.

6 Task 4: The free-vibrations problem

This task is used to introduce the dynamic forces in our problem. The main objective is to obtain the vibration modes of the wing according to the kinematic proposed in Task 1, consequently no aerodynamic forces will be involved at this stage, leaving them for the next tasks. In order to attempt the objectives, the following items must be solved

1. Deduce the mass matrix of the wing, $\mathbf{M}$.
2. Obtain the free motion equations and calculate the natural frequencies and mode shapes

6.1 The mass matrix

We assume the wing vibrating with relative low amplitudes. Thus, since the rotation angle w/b_0, $\theta \ll 1$, each point of the airfoil has approximately the same vertical displacement as its projection on the middle plane, already calculated in Task 1, Eq. (10). We rewrite that expression here but highlighting the time-dependence of dofs

$$z(x, y, t) = w(y, t) - x\,\theta(y, t) \equiv b_0\,\mathbf{N}_z^T(\xi, \eta)\mathbf{u}(t) \tag{40}$$

In dynamic systems, in the Lagrange equations the kinetic energy, $\mathcal{T}$, must be included and it should be evaluated as function of dofs $\mathbf{u}(t)$. Since we can approximate the wing as a plane surface $z(x, y, t)$, we can easily deduce the kinetic energy of a single point at (x, y) of mass dm as $d\mathcal{T} = \frac{1}{2}\dot{z}^2(x, y, t)\,dm$, where $\dot{z}$ is its vertical velocity (and unique, since no horizontal velocities are considered). The total kinetic energy of the wing will be

$$\mathcal{T} = \frac{1}{2}\int_{\mathcal{M}} \dot{z}^2(x, y, t)\,dm \tag{41}$$

where the 2D-integration domain can be mathematically expressed as

$$\mathcal{M} = \{(x, y) \in \mathbb{R}^2 : -b(y) \leq x \leq +b(y)\,,\ 0 \leq y \leq l\} \tag{42}$$

or in non-dimensional form

$$\mathcal{M} = \{(\xi, \eta) \in \mathbb{R}^2 : -b(\eta)/b_0 \leq \xi \leq +b(\eta)/b_0\,,\ 0 \leq \eta \leq 1\} \tag{43}$$

In order to complete the integration we need the density per unit-area, which is denoted by $\rho_s(\xi, \eta)$ and it is (in general) variable with the point. The function $\rho_s(\xi, \eta)$ expresses how distributed is the mass in the wing and it will be assumed as known. The mass element is then

$$dm = \rho_s(x, y)\, dx\, dy = b_0\, l\, \rho_s(\xi, \eta)\, d\xi\, d\eta \tag{44}$$

After introducing Eqs. (40), (44) in Eq. (41) and using the property shown in Task 1 to derive matrix expressions, we obtain

$$\begin{aligned}
\mathcal{T} &= \frac{1}{2}\int_{\mathcal{M}} \dot{z}^2(x, y, t)\, dm = \frac{1}{2}\int_{\mathcal{M}} \dot{z}^T\, \dot{z}\, dm \\
&= \frac{1}{2}\int_{\mathcal{M}} b_0^3 l \dot{\mathbf{u}}^T\, \mathbf{N}_z(\xi, \eta)\mathbf{N}_z^T(\xi, \eta)\, \dot{\mathbf{u}}\, \rho_s(\xi, \eta)\, d\xi\, d\eta \\
&= \frac{1}{2}\dot{\mathbf{u}}^T \left(b_0^3 l \int_{\mathcal{M}} \mathbf{N}_z(\xi, \eta)\mathbf{N}_z^T(\xi, \eta)\, \rho_s(\xi, \eta)\, d\xi\, d\eta \right) \dot{\mathbf{u}} \equiv \frac{1}{2}\dot{\mathbf{u}}^T\, \mathbf{M}\, \dot{\mathbf{u}}
\end{aligned}$$

The mass matrix will be then the result of integrating in the $\mathcal{M}$ domain

$$\mathbf{M} = b_0^3 l \int_{\mathcal{M}} \mathbf{N}_z(\xi, \eta)\mathbf{N}_z^T(\xi, \eta)\, \rho_s(\xi, \eta)\, d\xi\, d\eta \tag{45}$$

6.2 Eigenfrequencies and mode shapes of the wing

The natural frequencies and mode shapes of a vibrating structure together with their physical insight are maybe the most important concepts that students should acquire in a course of mechanical vibrations. In flight, the free-motion vibrations are modified by the aerodynamic conditions, but essentially the differential equations describing the oscillations are the same since they include mass, stiffness and dissipative matrices, although affected by the flow velocity. The Lagrange equations are again the starting point, but written now under their most general expressions, including inertial and dissipative terms (García-Fogeda & Sanz-Andrés, 2014; Dowell, 2005).

$$\frac{d}{dt}\left(\frac{\partial \mathcal{T}}{\partial \dot{\mathbf{u}}}\right) + \frac{\partial \mathcal{D}}{\partial \dot{\mathbf{u}}} + \frac{\partial \mathcal{U}}{\partial \mathbf{u}} = \mathbf{Q}(\mathbf{u}, \dot{\mathbf{u}}, \ddot{\mathbf{u}}) \tag{46}$$

where

$\mathcal{T}$: Kinetic energy of the system, expressed in general as a quadratic form of the dofs velocities $\mathcal{T} = \dot{\mathbf{u}}^T\mathbf{M}\dot{\mathbf{u}}/2$, with $\mathbf{M}$ the mass matrix.

$\mathcal{U}$: Strain energy of the system, expressed in general as a quadratic form of the dofs $\mathcal{U} = \mathbf{u}^T\mathbf{K}\mathbf{u}/2$ with $\mathbf{M}$ the mass matrix.

$\mathcal{D}$: Rayleigh dissipative potential, expressed in general as a quadratic form of the dofs velocities $\mathcal{D} = \dot{\mathbf{u}}^T\mathbf{D}\dot{\mathbf{u}}/2$ with $\mathbf{D}$ the damping matrix.

$\mathbf{Q}$: Generalized aerodynamic forces associated to $\mathbf{u}$. In general depending on the dofs, their velocities and accelerations. They will be derived in the next point (Task 5).

Using the aforementioned property in Eq. (23) for calculating the gradient operator $\partial/\partial\mathbf{u}$ of the quadratic forms, Eq. (46) leads to

$$\mathbf{M}\ddot{\mathbf{u}} + \mathbf{D}\dot{\mathbf{u}} + \mathbf{K}\mathbf{u} = \mathbf{Q}(\mathbf{u}, \dot{\mathbf{u}}, \ddot{\mathbf{u}}) \tag{47}$$

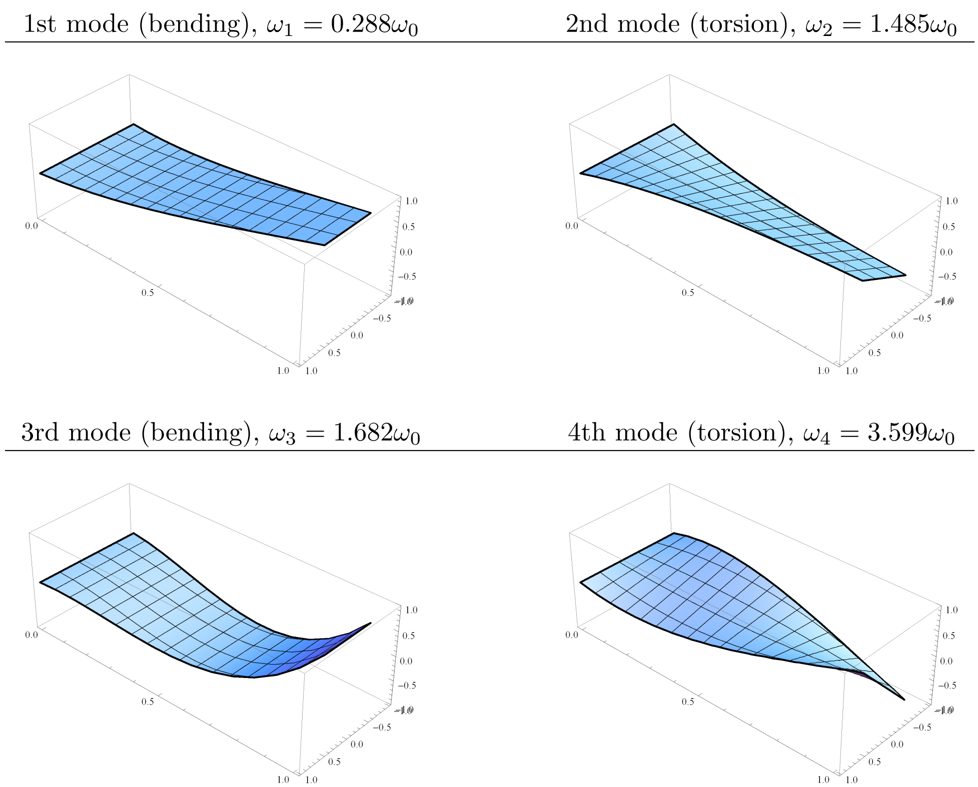

Figure 6: Undamped on-ground vibrating modes and associated natural natural frequencies refered to $\omega_0 = \sqrt{GJ/mb_0^3}$ for $EI = 0.9GJ$ and $l = 6b_0$

In this task we are interested in the undamped natural frequencies on ground (no aerodynamic forces are considered). Therefore, the free motion equation arise doing $\mathbf{D} = \mathbf{0}$ and $\mathbf{Q} = \mathbf{0}$ above, resulting classic mass-stiffness eigenvalue problem to extract the natural frequencies and modes

$$\mathbf{M}\ddot{\mathbf{u}} + \mathbf{K}\mathbf{u} = \mathbf{0} \tag{48}$$

Checking harmonic solutions of the form $\mathbf{u}(t) = \boldsymbol{\phi}\, e^{i\omega t}$, the natural frequencies and the mode shapes are the solutions ω, $\boldsymbol{\phi}$ of the eigenvalue problem

$$\left[-\omega^2\mathbf{M} + \mathbf{K}\right]\boldsymbol{\phi} = \mathbf{0} \tag{49}$$

Students are able to solve this problem using the software Wolfram Mathematica©. However, the obtained modes $\{\boldsymbol{\phi}_j\}_{j=1}^{4}$ has not in appearance physical significance. In order to visualize the 3D deformation due to each mode, we use the Eq. (40), which transforms the dofs into the deformed surface. This allows to detect the nature of each mode: bending and torsion. The results of mode shapes and natural frequencies are shown in Fig. (6). Using the `Manipulate` command of Mathematica we can animating the modes according to the associated frequency.

7 Task 5: Dynamic aeroelasticity (I): unsteady aerodynamics

To compute the lift pressure balance in an airfoil under incompressible subsonic flow is beyond the scope of this paper. We will use instead the main results on unsteady aerodynamics, that is, the expressions of unsteady lift-force L and pitch-moment M on an airfoil undergoing heave w and pitch θ motion. Considering known the expressions of $L(y,t)$ and $M(y,t)$ as function of heave and pitch motion, their velocity and accelerations, the objective is to deduce the generalized forces associated to $\mathbf{u}$. This will be addressed in two stages

1. Express lift $L(\eta,t)$ and pitch moment $M(\eta,t)$ as function of degrees of freedom array $\mathbf{u}$.
2. Obtain the generalized forces associated to $\mathbf{u}$ assuming unsteady incompressible flow.

7.1 Lift and pitch moment

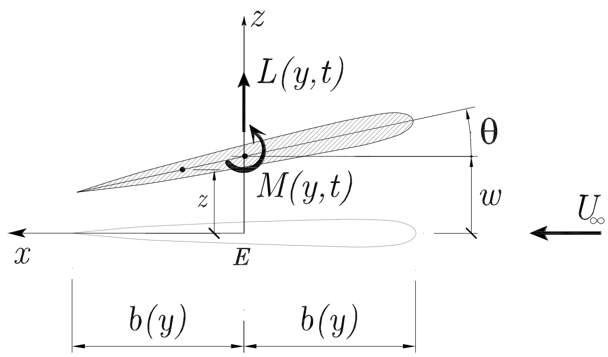

Figure 7: Lift and moment forces on the airfoil located at y coordinate

Consider a 2D airfoil within a constant horizontal flow with velocity U_∞, which also undergoes transverse motion. The aerodynamic conditions are changing at every time and consequently, the pressure distribution also varies. Assuming incompressible potential flow and under low amplitude harmonic vibrations of frequency ω, analytical expressions of the lift pressure coefficient can be derived. The basis of this derivation is of a great didactic relevance, since new concepts related with unsteady aerodynamics are introduced as unsteady circulation, unsteady boundary conditions and effects on airfoil due to vortex distribution along the weak (Gülçat, 2010; Bisplinghoff & Ashley, 1962; Fung, 1993). However, mathematically the obtained expressions as function of boundary conditions are not manageable due to not easily solvable integrals involved. For the particular case of heave $w(t)$ and pitch $\theta(t)$ harmonic motion of frequency ω, close expressions are available by integration of lift pressure coefficient along the chord. Thus, our wing can be considered as a infinite set of airfoils placed in parallel along the span, assuming that there is no aerodynamic influence between an airfoil and the rest (valid for large wing span). The lift force $L(y,t)$ and pitch moment $M(y,t)$ per unit-length at the center $(x=0)$ of the airfoil located at coordinate y, with semi-chord $b=b(y)$ and undergoing heave and pitch motion, $w(y,t)$ and $\theta(y,t)$ is (see Fig. 7)

$$\begin{aligned} L(y,t) &= \pi\rho_\infty b^2\left(-\ddot{w}+U_\infty\dot{\theta}\right)+2\pi\rho_\infty U_\infty b\,\mathcal{C}(\kappa)\left(-\dot{w}+U_\infty\theta+\frac{b}{2}\dot{\theta}\right) \\ M(y,t) &= -\pi\rho_\infty b^3\left(\frac{1}{2}U_\infty\dot{\theta}+\frac{b}{8}\ddot{\theta}\right)+\pi\rho_\infty U_\infty b^2\,\mathcal{C}(\kappa)\left(-\dot{w}+U_\infty\theta+\frac{b}{2}\dot{\theta}\right) \end{aligned} \tag{50}$$

where ρ_∞ is the air density and $b = b(\eta) \equiv b_0\,\psi(\eta)$ is the semi-chord, assumed variable within the span through the function $\psi(\eta)$. For example, if chord varies linearly from $2b_0$ to b_0, than $\psi(\eta) = (1 - \eta/2)$. The function

$$\mathcal{C}(\kappa) = \frac{H_1^{(2)}(\kappa)}{H_1^{(2)}(\kappa) + i\,H_0^{(2)}(\kappa)}$$

is the well known Theodorsen function, expressed in terms of Hankel functions and depending on the airfoil reduced frequency $\kappa = \frac{\omega b}{U_\infty}$. Not that this latter depends on the y coordinate via b, leading to evident computational difficulties. Analytical solutions can only be obtained assuming that $\mathcal{C}(\kappa)$ does not depend on y, avoiding in this way its integration along the span. For that, we consider that the reduced frequency inside Theodorsen function is

$$\kappa = \frac{\omega b_r}{U_\infty}$$

where b_r is the semi-chord of certain representative airfoil of the wing, located at a distance between $0.2l$ and $0.3l$ from the wingtip (Bisplinghoff & Ashley, 1962). It can be easily proved that κ is the relationship between the oscillation period and the time taken by the airfoil to cover a distance $2b$ in horizontal. Another consequence of the unsteady aerodynamics theory is that κ is closely related with the influence of the wake vortex on the airfoil. Thus, if $\kappa \ll 1$ the airfoil oscillates relatively slower than its horizontal velocity. Intuitively, a vortex shed at certain time will lay far from the airfoil at the next oscillation, so that its influence on the pressure distribution will be relatively low. Mathematically this is directly related with the values of the Theodorsen function, verifying $\mathcal{C}(\kappa) \to 1$ when $\kappa \to 0$. In this case, the value $\mathcal{C}(\kappa) \approx 1$ can be substituted in Eq. (50) avoiding the κ dependence of equations, leading to the usually named *quasi-steady aerodynamic models*. In contrast, for high oscillation frequencies respect to the flow velocity, the dependence on the reduced frequency can not be neglected and the problem should be solved including the effect of the weak via $\mathcal{C}(\kappa)$. More details on the derivation of Eqs. (50) can be found in references (Gülçat, 2010; Dowell, 2005).

7.2 Unsteady Generalized forces

The challenge of this task is to deduce a compact expression for the generalized forces $\mathbf{Q}$ of the entire wing from the airfoil aeordynamic forces, Eqs. (50), and from the kinematics, given by Eqs. (7),(8), highlighting the dependence on the dofs, their velocities and accelerations, $\mathbf{u}$, $\dot{\mathbf{u}}$, $\ddot{\mathbf{u}}$. The problem will be addressed in three different stages

Stage 1. Kinematic array $\mathbf{v}(\eta, t)$

The kinematic variables of any airfoil located at $y = \eta l$ can be grouped in a vector $\mathbf{v}(\eta, t) = \{w(\eta, t)/b_0, \theta(\eta, t)\}^T$, directly related with the dofs of the structure via η-dependent matrix $\mathbf{H}(\eta)$

$$\mathbf{v}(\eta, t) = \left\{ \begin{array}{c} w(\eta, t)/b_0 \\ \theta(\eta, t) \end{array} \right\} = \mathbf{H}(\eta)\,\mathbf{u}(t) \tag{51}$$

The entrees of matrix $\mathbf{H}(\eta) \in \mathbb{R}^{2\times 4}$ can easily be deduced from the shape functions, Eqs. (7),(8), obtained in Task 1.

Stage 2. Forces array $\mathbf{q}(\eta, t)$

As before, but now in terms of forces, the unsteady arodynamic lift and moment of any airfoil located at $y = \eta l$ can be written in vector form in the array $\mathbf{q}(\eta, t) = \{L(\eta, t)\, b_0, M(\eta, t)\}^T$. From Eqs. (50), it can be derived the expression

$$\mathbf{q}(\eta, t) = \rho_\infty U_\infty^2\, \mathbf{A}_0(\eta)\, \mathbf{u} + \rho_\infty U_\infty\, \mathbf{B}_0(\eta)\, \dot{\mathbf{u}} + \rho_\infty\, \mathbf{C}_0(\eta)\, \ddot{\mathbf{u}} \tag{52}$$

where matrices $\mathbf{A}_0(\eta), \mathbf{B}_0(\eta), \mathbf{C}_0(\eta) \in \mathbb{R}^{2\times 4}$ can be obtained identifying terms in $w, \dot{w}, \ddot{w}, \theta, \dot{\theta}, \ddot{\theta}$ in Eqs. (50) and using Eq. (51) for the transformation into the dofs.

Stage 3. Generalized forces $\mathbf{Q}(t)$

Let us consider a virtual variation on the dofs, $\delta\mathbf{u}$. Heave and pitch variation of each section y is then

$$\delta w(\eta, t) = b_0\, \mathbf{N}_w^T(\eta)\, \delta\mathbf{u}(t) \quad , \quad \delta\theta(\eta, t) = \mathbf{N}_\theta^T(\eta)\, \delta\mathbf{u}(t) \tag{53}$$

Therefore, the total virtual work made by aerodynamic forces along the entire span is

$$\delta\mathcal{W} = \int_{y=0}^{l} L(y, t)\, \delta w\, dy + \int_{y=0}^{l} M(y, t)\, \delta\theta\, dy \tag{54}$$

This (scalar) expression can be written in terms of the above defined magnitudes $\mathbf{v}$ and $\mathbf{q}$ as

$$\delta\mathcal{W} = \int_{y=0}^{l} \{\delta w/b_0, \delta\theta\} \left\{ \begin{array}{c} L(y,t)b_0 \\ M(y,t) \end{array} \right\} dy = \int_{y=0}^{l} \delta\mathbf{v}^T(y,t)\, \mathbf{q}(y,t) dy \tag{55}$$

Finally, using Eqs. (51) and (52) we have

$$\begin{aligned} \delta\mathcal{W} &= \delta\mathbf{u}^T \int_{\eta=0}^{1} l\, \mathbf{H}^T(\eta) \left[\rho_\infty U_\infty^2\, \mathbf{A}_0(\eta)\, \mathbf{u} + \rho_\infty U_\infty\, \mathbf{B}_0(\eta)\, \dot{\mathbf{u}} + \rho_\infty\, \mathbf{C}_0(\eta)\, \ddot{\mathbf{u}}\right] d\eta \\ &\equiv \delta\mathbf{u}^T \left(\rho_\infty U_\infty^2 \mathbf{A}\mathbf{u} + \rho_\infty U_\infty \mathbf{B}\dot{\mathbf{u}} + \rho_\infty \mathbf{C}\ddot{\mathbf{u}}\right) \equiv \delta\mathbf{u}^T \mathbf{Q}(t) \end{aligned} \tag{56}$$

where

$$\mathbf{A} = l \int_{\eta=0}^{1} \mathbf{H}^T(\eta)\mathbf{A}_0(\eta) d\eta\ ,\ \mathbf{B} = l \int_{\eta=0}^{1} \mathbf{H}^T(\eta)\mathbf{B}_0(\eta) d\eta\ ,\ \mathbf{C} = l \int_{\eta=0}^{1} \mathbf{H}^T(\eta)\mathbf{C}_0(\eta) d\eta \tag{57}$$

and

$$\mathbf{Q}(t) = \rho_\infty U_\infty^2 \mathbf{A}\, \mathbf{u} + \rho_\infty U_\infty \mathbf{B}\, \dot{\mathbf{u}} + \rho_\infty \mathbf{C}\, \ddot{\mathbf{u}} \tag{58}$$

Note that the generalized forces depend explicitly on the dofs, their velocity and acceleration. The three matrices have size 4×4 and in general will depend additionally on the reduced frequency κ. In fact, only $\mathbf{A}$ and $\mathbf{B}$ are function of κ, because aerodynamic forces due to accelerations $\ddot{w}$ and $\ddot{\theta}$ are independent on the reduced frequency, something that can be deduced by simple observation of terms multiplied by $\mathcal{C}(\kappa)$ in Eq. (50). The integrals shown in Eq. (57) can be easily computed using the symbolic software Wolfram Mathematica© as in the previous tasks.

8 Task 6: Dynamic aeroelasticity (II): flutter instability

The different parts of the Lagrange mechanics equations have been separately obtained in matrix form in the previous tasks: kinematic energy, strain energy, dissipative potential and generalized forces. Now, in this task we will derive the motion equations, that as we will be shown, results a homogeneous system of time linear differential equations. Thus, we can apply the modal analysis to extract the eigenfrequencies and eigenmodes for each regime velocity U_∞. The information of the stability of any dynamical system is collected through the analysis of the eigenvalues, that is the complex frequencies. The main objective of this task is the learning and insight of a non trivial concept: the aeroelastic flutter. For that we follow these two points.

1. Deduce the motion equations and the eigenvalue problem to obtain the flutter curves.
2. Solve numerically the flutter problem for different cases, interpreting the results.

8.1 The motion equations and the flutter problem

In Task 5, the expression of generalized aerodynamic forces for incompressible potential flow with horizontal velocity U_∞ has been derived. The general form of Lagrange equations for vibrating systems have already been introduced in Task 4, Eqs. (46),(48). Introducing in them the results for $\mathbf{Q}$ given by Eq. (56) we have

$$\begin{aligned} \frac{d}{dt}\left(\frac{\partial \mathcal{T}}{\partial \dot{\mathbf{u}}}\right) + \frac{\partial \mathcal{D}}{\partial \dot{\mathbf{u}}} + \frac{\partial \mathcal{U}}{\partial \mathbf{u}} &= \mathbf{Q}(\mathbf{u}, \dot{\mathbf{u}}, \ddot{\mathbf{u}}) \\ \mathbf{M}\ddot{\mathbf{u}} + \mathbf{D}\,\dot{\mathbf{u}} + \mathbf{K}\mathbf{u} &= \rho_\infty U_\infty^2 \mathbf{A}\mathbf{u} + \rho_\infty U_\infty \mathbf{B}\dot{\mathbf{u}} + \rho_\infty \mathbf{C}\ddot{\mathbf{u}} \end{aligned} \tag{59}$$

Grouping terms in $\mathbf{u}$, $\dot{\mathbf{u}}$ and $\ddot{\mathbf{u}}$

$$(\mathbf{M} - \rho_\infty \mathbf{C})\,\ddot{\mathbf{u}} + (\mathbf{D} - \rho_\infty U_\infty \mathbf{B})\,\dot{\mathbf{u}} + \left(\mathbf{K} - \rho_\infty U_\infty^2 \mathbf{A}\right)\mathbf{u} = \mathbf{0} \tag{60}$$

If we name

$$\mathbf{M}_{eq} = \mathbf{M} - \rho_\infty \mathbf{C}\ ,\ \mathbf{D}_{eq}(U_\infty) = \mathbf{D} - \rho_\infty U_\infty \mathbf{B}\ ,\ \mathbf{K}_{eq}(U_\infty) = \mathbf{K} - \rho_\infty U_\infty^2 \mathbf{A} \tag{61}$$

then the homogeneous system of differential equations adopts the form

$$\mathbf{M}_{eq}\ddot{\mathbf{u}} + \mathbf{D}_{eq}(U_\infty)\,\dot{\mathbf{u}} + \mathbf{K}_{eq}(U_\infty)\,\mathbf{u} = \mathbf{0} \tag{62}$$

These equations govern the unforced-damped vibrations of the wing for certain flight velocity U_∞. Somehow, the aerodynamic conditions change the dynamic matrices: mass, damping and stiffness. Thus, while damping and stiffness matrices are modified with flow velocity, mass matrix also changes due to the presence of air, although does not depend on the velocity. In fact, the two terms of $\mathbf{M}_{eq}$ represent the mass matrix of the wing structure and the mass matrix of the air around the airfoil.

Like any vibrating system under free motion, the solution Eqs. (62) can be written in terms of the complex eigenfrequencies and their associated complex modes. The eigenvalue problem to obtain these frequencies can be derived checking solutions of the form $\mathbf{u}(t) = \bar{\mathbf{u}}\, e^{i\omega t}$, resulting

$$\left[-\omega^2 \mathbf{M}_{eq} + i\omega\, \mathbf{D}_{eq}(U_\infty) + \mathbf{K}_{eq}(U_\infty)\right]\bar{\mathbf{u}} = \mathbf{0} \tag{63}$$

Non-trivial solutions of $\bar{\mathbf{u}}$ are those associated to the values of ω verifying the equation

$$\det\left[-\omega^2 \mathbf{M}_{eq} + i\omega\, \mathbf{D}_{eq}(U_\infty) + \mathbf{K}_{eq}(U_\infty)\right]\bar{\mathbf{u}} = \mathbf{0} \tag{64}$$

This equation defines the set of complex frequencies as functions of the velocity U_∞, considered now as a variable parameter. In fact, theoretically, solving repeatedly the Eq. (64) for a list of values assigned to U_∞, we can obtain the evolution of the complex frequencies with the flight velocity. Let us denote $\omega_j(U_\infty) = \Omega_j + i\, g_j \in \mathbb{C}$ and $\mathbf{u}_j \in \mathbb{C}^4$ to one (any) of these frequencies and its complex associated eigenvector, respectively. Although not shown, both Ω_j and g_j are functions of the velocity U_∞. The curves which represent the variation $\Omega_j(U_\infty)$ are usually named $V\omega$ curves while $g_j(U_\infty)$ are named Vg curves. The general solution of free-motion vibrations can be considered as a superposition of the complex modes, thus in the expression of $\mathbf{u}(t)$ there exists a term proportional to the jth mode. Mathematically, there exists a coefficient $c_j \in \mathbb{C}$ such that

$$\mathbf{u}(t) = \cdots + c_j\, \mathbf{u}_j\, e^{i\,\omega_j t} + \cdots \tag{65}$$

where the rest of terms associated to the others complex modes have been omitted. Replacing $\omega_j = \Omega_j + i g_j$

$$\begin{aligned} \mathbf{u}(t) &= \cdots + c_j\, \mathbf{u}_j\, e^{i\,(\Omega_j + i g_j)t} + \cdots \\ &= \cdots + c_j\, \mathbf{u}_j\, e^{i\,\Omega_j t}\, e^{-g_j t} + \cdots \\ &= \cdots + c_j\, \mathbf{u}_j\, e^{-g_j t}\,(\cos \Omega_j t + i\, \sin \Omega_j t) + \cdots \end{aligned} \tag{66}$$

At first sight, we observe that the solution is harmonic with an *exponentially decreasing amplitude*. However, this affirmation (*decreasing*) is valid only if $g_j > 0$. In our problem, the imaginary part is variable with U_∞, so that it could exist (as in fact it occurs) certain velocity range where $g_j < 0$. Within this range, the imaginary part can be written as $g_j = -|g_j|$ and the associated amplitudes to the jth mode are now exponentially increasing since they are multiplied by $e^{|g_j|t}$. Consequently in this flight regime the vibrations become unstable and the structure will collapse. This phenomenon is known as *flutter*. Due to the consequences of flutter to know a priori (or at least to approach) the critical velocity limiting stable and unstable vibrations is of capital importance. This is known as *flutter velocity*, denoted by U_f, and characterized by being the lowest velocity which verifies simultaneously the following three properties, for some mode j:

$$(i)\ g_j(U_f - \epsilon) \geq 0\ , \quad (ii)\ g_j(U_f) = 0\ , \quad (iii)\ g_j(U_f + \epsilon) < 0\ , \tag{67}$$

The real part of the complex frequency at the flutter velocity $\Omega_f = \Omega_j(U_f)$ is named the *flutter frequency*. If the flutter frequency is also null, $\Omega_f = 0$, then the instability occurs in absence of vibrations. The obtained critical velocity is then called *divergence velocity*, already studied in the Task 3. To a better understanding of this phenomenon instability, the flutter curves $V\omega$ and Vg should be plotted.

8.2 Flutter curves

We think that the main challenge in the teaching of dynamic aeroelasticity are to get students to learn the physical insight of flutter and to read the flutter curves. To solve the nonlinear eigenvalue problem of Eq. (63) we use the named k-method (Wright & Cooper, 2007). However, to explain the details of this method is beyond of the scope of this task and consequently of this paper. The students have separately obtained along the previous tasks the different matrices involved in this equation. They are not required to program the k-method in this task, however the should know how to use it. The scripts of the k-method are provided by the teacher in Matlab m-files, taking as input the calculated matrices and getting as output the flutter (dimensionless) curves. The objective is to represent these curves and visualizing

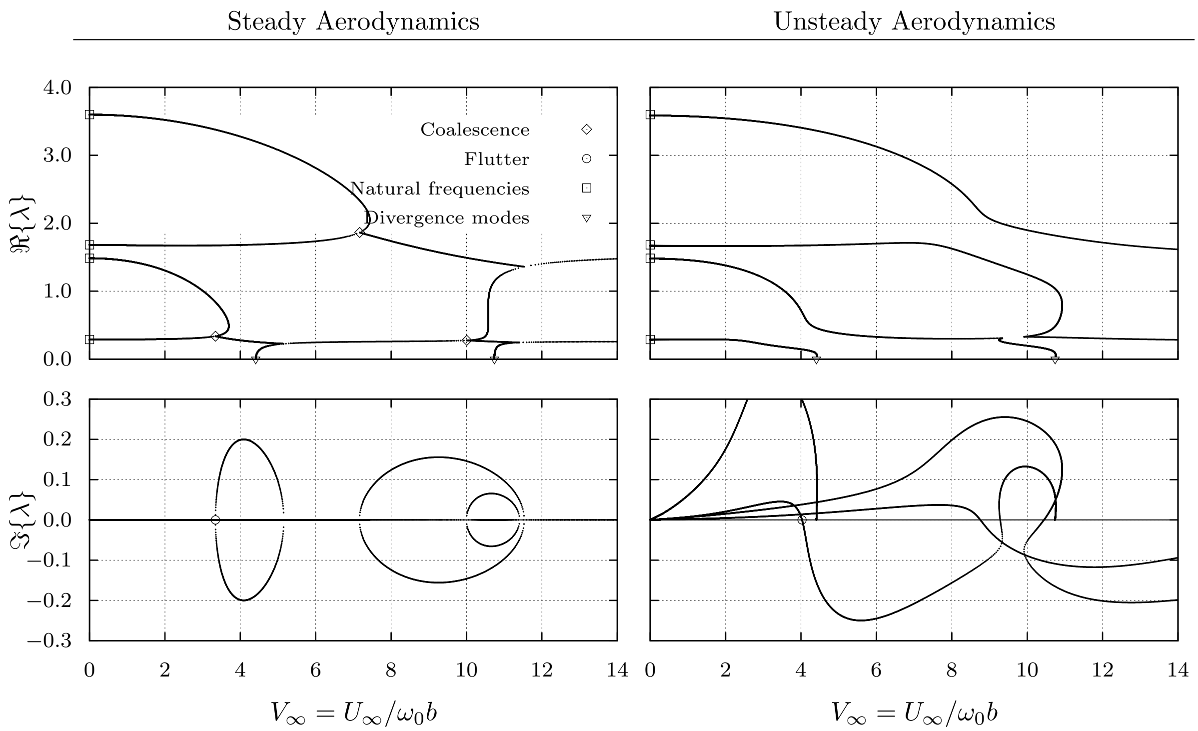

Figure 8: Frequencies ($V\omega$ plots, top) and damping ratio (Vg plots, bottom) calculated for the 4 dof finite element model and for two aerodynamic models (steady and unsteady)

how both the real and imaginary part of complex eigenvalues (also just named *frequency* and *damping ratio* respectively) depend on the following parameters

- The relationship between the wing and air masses
- The relative position between center of gravity and flexural axis
- The inherent dissipative capability of the structure, given by matrix $\mathbf{D}$.
- The type of considered aerodynamic forces: steady ($\mathbf{A} \neq \mathbf{0}$, $\mathbf{B} = \mathbf{0}$, $\mathbf{C} = \mathbf{0}$) or unsteady ($\mathbf{A} \neq \mathbf{0}$, $\mathbf{B} \neq \mathbf{0}$, $\mathbf{C} \neq \mathbf{0}$)

A complete description of the influence of these parameters can be found in the reference (Wright & Cooper, 2007). As an example, in Fig. 8 the flutter curves obtained by the students for certain values of the given parameters have been plotted. The obtained results under steady and unsteady aerodynamics have been separated, due to their particular interest. We highlight here the most relevant information given by these curves.

Fig. 8(left) shows the $V\omega$(top) and Vg(bottom) curves calculated using a purely steady aerodynamic model, that is the generalized forces calculated in Eq. (56) are reduced to $\mathbf{Q} = \rho_\infty U_\infty^2 \mathbf{A}\mathbf{u}$. This case has an special interest since the modal coupling (also called *coalescence*) can clearly be observed. This phenomenon is the merge at a point of the real parts for torsional and bending modes. Mathematically, it can be proved that this point matches with a bifurcation in the imaginary part, producing instability (flutter). This is the behavior followed by the 2nd and 4th modes (torsional modes) in $V\omega$ plot when they merge with the bending modes (1st and 3rd modes). Flutter for steady aerodynamics is always related to bifurcation points (matching coalescence with flutter) so that the general aspect of the flutter curves is like those ones plotted in Figs. 8(left). For this reason, the phenomenon is sometimes referred as modal coupling instability, since more than one mode must be involved. Note that the flutter is the lowest velocity associated to bifurcation points in the imaginary part.

In Fig. 8(right) the frequency and the damping ratio trends for unsteady aerodynamics are represented. We observe four curves in each plot, corresponding to the four computed modes (remember that our finite element model have four dofs). One of the damping ratio curves crosses the horizontal axis approximately at $U_f \approx 4\omega_0 b_0$, point which defines the flutter critical velocity. Although now pure modal coupling is not observed, the real parts of torsional and bending frequencies are approaching each other around the flutter velocity. Additional information is provided by these plots, thus for example the two divergence modes can be perceived as those velocities for which the frequency vanishes (both real and imaginary part).

9 Conclusions

In this paper, the aeroelastic problem of a 3D-wing applying the finite element method is presented. Due to apparent complexity of the problem, we propose to divide the work in six tasks. In each task, the basis of the following one are settled so that at the last one (task 6) we can solve one of the most important problems in aeroelasticiy: flutter instability. In addition, each task allows to analyze individual problems as structural deformation, the divergence instability, free vibrations, etc,...always from a discrete point of view, using a finite element model. In this paper we have presented the learning methodology mainly based on the systematic use of matrix expressions that allow the generalization of the method for a larger number of degrees of freedom. The tasks are carried out at the same time that the theoretical lessons, so that the students can practice the acquired concepts on a more complex system with four degrees of freedom. This latter, together with the merge of different areas (finite elements, mechanics, vibrations, structures) stimulate the students, getting in general a high satisfaction level.

Modelling in Science Education and Learning
http://polipapers.upv.es/index.php/MSEL

References

Balakrishnan, A. V. (2012).
Fundamentals of aerodynamics.
McGraw-Hill.

Anderson, J. D. (2001).
Aeroelasticity: the continuum theory.
Springer.

Bisplinghoff, R. L., & Ashley, H. (1962).
Principles of aeroelasticity.
Dover Publications.

Dowell, E. H. (2005).
A modern course in aeroelasticity (E. H. Dowell, Ed.).
Kluwer Academic Publishers.

Edwards, J., & Wieseman, C. (2008).
Flutter and divergence analysis using the generalized aeroelastic analysis method.
Journal of Aircraft , 45 (3), 906–915.

Fung, Y. C. (1993).
An introduction to the theory of aeroelasticity.
Dover Publications.

García-Fogeda, P., & Sanz-Andrés, A. (2014).
Introducción a las vibraciones.
Garceta Grupo Editorial.

Gülçat, U. (2010).
Fundamentals of modern unsteady aerodynamics.
Springer.

Hancock, G., Wright, J., & Simpson, A. (1985).
On the teaching of the principles of wing flexure-torsion flutter.
Aeronautical Journal , 89 (888), 285–305.

Megson, T. (2010).
An introduction to aircraft structural analysis.
Butterworth-Heinemann.

Meseguer, J., & Sanz-Andrés, A. (2010).
Aerodinémica básica.
Garceta Grupo Editorial.

Wright, J. R., & Cooper, J. E. (2007).
Introduction to Aircraft Aeroelasticity and Loads.
John Wiley & Sons.

Zienkiewicz, O., & Taylor, R. (2005).
The Finite Element Method. 1-Basis.
Butterworth Heinemann.

Modelling in Science Education and Learning
http://polipapers.upv.es/index.php/MSEL